XIX IMEKO World Congress
Fundamental and Applied Metrology
September 6−11, 2009, Lisbon, Portugal

FUNDAMENTAL VERIFICATION FOR 2-DIMENSIONAL SUPER-RESOLUTION OPTICAL INSPECTION FOR SEMICONDUCTOR DEFECTS BY USING STANDING WAVE ILLUMINATION SHIFT

R. Kudo [1], *S. Usuki* [2], *S. Takahashi* [1] *and K. Takamasu*[1]

[1] Department of Precision Engineering, The University of Tokyo, 7-3-1 Hongo, Bunkyo-ku, Tokyo, JAPAN, honc@nanolab.t.u-tokyo.ac.jp
[2] Division of Global Research Leaders, Shizuoka University, 3-5-1 Johoku, Naka-ku, Hamamatsu, JAPAN, dsusuki@ipc.shizuoka.ac.jp

Abstract – Semiconductor design rules and process windows continue to shrink, and developing new processes to accommodate parameters such as less-than-50nm design rules and a 300mm wafer becomes increasingly challenging [1]. Next-generation defect inspection is urgently demanded. Optics and electron beams have been the main technologies for detection of the critical defects, but both have their disadvantages. Optical inspection is generally not sensitive enough for defects at 100nm geometries and below, while SEM inspection has low throughput because it takes a long time to scan 300mm. In order to find a solution to these problems, we propose a novel optical inspection method for critical defects on semiconductor wafers. Until now, 1-dimensional resolution beyond the Rayleigh limit has been theoretically studied and experimentally bought to realization by a method called super resolution [2,3]. To apply the proposed method to a sample with 2-dimensional structure, we have altered the proposed method making a standing wave shift in 2 directions, and carrying out super-resolution in each shifting direction. We carried out a fundamental verification of this method by computer simulation and experiment. As a result, we discovered the possibility of resolving a 2-dimensional structure which can't be resolved by the normal imaging system.

Keywords: standing wave illumination, image reconstruction, super-resolution

1. INTRODUCTION

According to the ITRS roadmap [1], a next-generation semiconductor defect inspection system is urgently demanded, and the challenges for defect detection increase exponentially with shrinking design, such as sub-100-nm nodes. One of the key areas where improvement is needed is defect detection of semiconductor wafers [4]. Defects in the wafers include random defects like killer particles, clustered defects, scratch defects and so on. These defects deteriorate electrical chip performance and process yield in the semiconductor manufacturing process. Especially, improved inspection of patterned wafers is a necessity for the next generation of semiconductors.

Optical methods and electron beams are conventionally used for semiconductor wafer inspection [5]. However, with the continuous miniaturization of interconnects, optical inspection becomes less useful because of its diffraction limit. On the other hand, electron beams lack utility for wider wafer inspection because of their low throughput property. We think optical inspection has greater potential than SEM inspection for inspection under the less-than-50nm design rule and 300mm wafers because optical inspection is non-destructive and has high throughput. So, we focused our attention on optical inspection. In optical wafer inspection, resolution and defect detection beyond the Rayleigh limit are now required due to the acceleration of pattern miniaturization and development of advanced semiconductor devices [6].

One of the solutions to challenges in semiconductor optical inspection is the use of shorter wavelengths, which has been studied as a countermeasure against device miniaturization. However, as the shortening of wavelength is too limited to keep up with the challenges, we have developed a super-resolution inspection technique. Namely, when a pattern is miniaturized and made dense, light reflected from the wafer becomes weak, and the captured image becomes dark with low contrast; hence, a high-sensitivity method that can obtain a lot of optical information must be developed [7]. Our super-resolution inspection technique combines a standing wave illumination shift method with dark-field imaging technology to deliver optimal sensitivity for critical defect detection at sub-100-nm nodes and beyond, without compromising throughput. The standing wave illumination shift method enables the optical resolution of patterns that the conventional method cannot achieve. Nano-scale shifts of illumination and super-resolution post-processing are keys to achieving the resolution enhancement and higher sensitivity for defect detection.

ISBN 978-963-88410-0-1

2. METHODOLOGY

2.1. Standing wave illumination shift and scattered light modulation

A schematic diagram of the standing wave illumination shift and the scattered light modulation is shown in Figure 1. The standing wave illumination is generated by 2-beam interference. The standing wave illumination is scattered by the sample surface, and the scattered light is focused on the CCD imaging surface through the imaging lens. The standing wave is shifted on a nanoscale by the phase difference between the 2 beams in the illumination (Fig. 1.(a)). Then, the scattered light is modulated by the shift of the standing wave illumination (Fig. 1. (b)). A super-resolution image of scattering efficiency can be calculated from multiple images by the super-resolution image reconstruction algorithm.

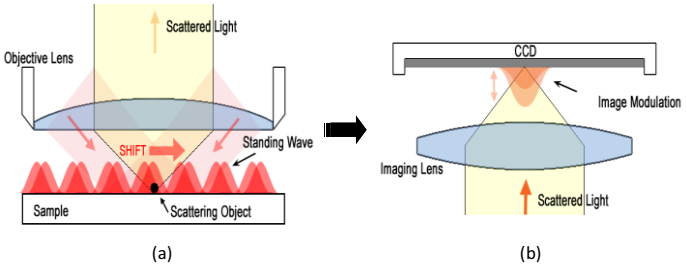

Fig. 1. Schematic diagram of the standing wave illumination shift and the scattered light modulation

2.2. Super-resolution image reconstruction algorithm for post processing

A block diagram of the super-resolution post-processing is shown in the Fig. 2. First, the sample is illuminated with standing wave illumination, and multiple images are experimentally observed by the standing wave shift. Then, calculated images are computationally obtained based on Fourier optics. The error between the observed images and the calculated images is approximately fed back to the assumed sample to obtain a reconstructed sample. The image reconstruction is iteratively calculated with successive approximation until the error converges. The nanoshifts of standing wave illumination that are modulated at about a half-wavelength scale include high-frequency spatial information, and this causes change to the scattered light images. We expect to achieve super resolution by feeding back the errors in scattered light images into sample distribution and reconstructing the sample distribution with successive approximation.

Fig. 3 shows the schematics of 1-dimensional (1D) super resolution. When two point samples to be observed are close enough (shown as two blue dots), the two points cannot be distinguished in the observed image. Then, the sample is illuminated by the standing wave, and multiple modulated scattered light images are obtained. These obtained images are post-,processed; then the two point samples are clearly resolved as shown in the lower right image. Thus, a super resolution is achieved.

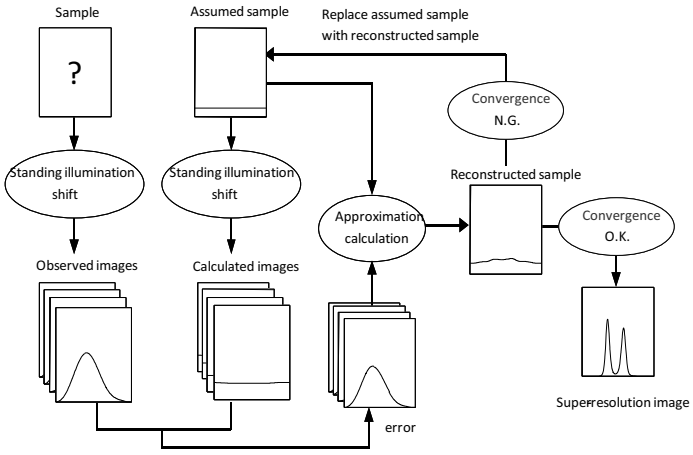

Fig. 2. Block diagram of the super-resolution post-processing

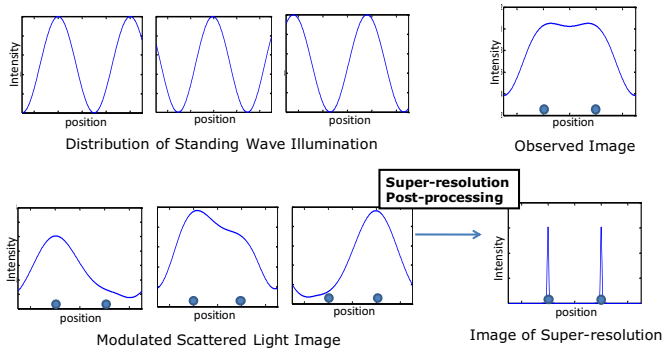

Fig. 3. The schematics of super-resolution (1D)

2.3. 2-direction standing wave illumination shift

Two-dimensional (2D) super-resolution reconstruction is put into practice by extending the method explained in the preceding section. 2D super-resolution is carried out by presuming a 2D map of scattering efficiency and applying the reconstruction algorithm to 1D domains (rows and columns) in order. In particular, a 2D super-resolution image is obtained using multiple images which are in turn sequentially obtained by shifting standing wave illumination in two directions each differing by an angle of 90 degrees to the sample. Alternating images from different angles are used to calculate sequential reconstruction (Fig. 4.).

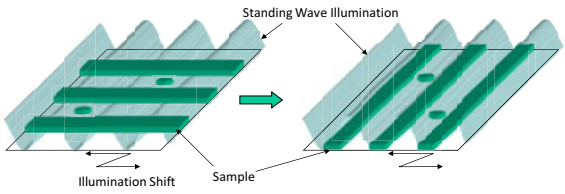

Fig. 4. 2-direction shift of standing wave illumination

3. 2D SUPER-RESOLUTION SIMULATION

3.1. 2D super-resolution simulation for discrete punctate scattered objects

To verify the feasibility of the 2D super-resolution method, a computer simulation based on Fourier optics was carried out. First, we attempted super resolution on a sample of discrete punctate scattered objects to investigate

the fundamental characteristics of 2D super resolution. The 2D super-resolution simulation setup is defined in Table 1.

Table 1. Simulation setup

Wavelength of source	488nm
Pitch of structured light illumination	300nm
NA of objective	0.95
Rayleigh limit	313nm
Shift times	10
Shift step size	30nm
Iteration tmes	1000

Here, particles 50nm in diameter are assumed as discrete punctuate scattered objects, and are put in random positions (Fig. 5). Fig. 5 (a) is the distribution of the assumed sample. Fig. 5 (b) is the normal microscopic image of uniform illumination: a bandwidth-limited image by *NA*. It is confirmed that the structure of the sample is not resolved in Fig. 5 (b).

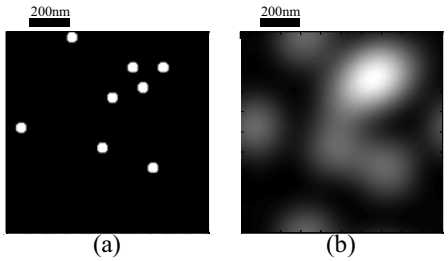

Fig. 5. (a) Discrete punctate scattered objects,
(b) Normal imaging of *NA*0.95

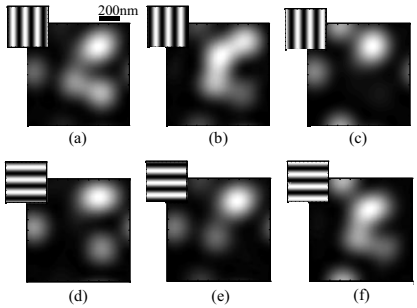

Fig. 6. Examples of modulated scattered light images by standing wave illumination shift

Examples of changing images by standing wave illumination shift are shown in Fig. 6. The smaller figures inset at the upper left corners show the directions of standing wave illumination. The larger figures show the sample images illuminated by the standing wave. As these figures show, standing wave illumination shifts in 2 directions, and for each direction of standing wave illumination, modulated images are obtained. Shifting illumination, and the illuminated part of the scattered objects changes, and we can see that the observed images are modulated. In none of the modulated figures, however, is the sample structure resolved.

In Fig. 7 we show the 2D super-resolution reconstructed image using the multiple images. The super-resolution image approximately corresponds to the sample; a structure that could not be resolved by uniform illumination is made distinguishable.

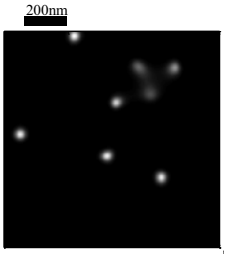

Fig. 7. The image of 2D super-resolution obtained by simulation

3.2. 2D super-resolution simulation for line & space pattern

In this section, 2D super-resolution simulation is carried out on another sample. The simulation setup is as defined in Table 1. Assuming an actual semi-conductor pattern, we set a sample which is a 100nm line & space (L&S) pattern and has multiple short circuits and broken wires (Fig. 8(a)). Fig. 8(b), which is the image by uniform illumination, shows only parts of high density of the object (short circuits) indistinctly, and the L&S pattern is not observed because 100nm is below the Rayleigh limit (313nm). On the other hand, in the super-resolution image (Fig. 9), the L&S pattern is reconstructed, and the position of short circuits and broken wires becomes clear. The possibility of defect inspection of an L&S pattern by 2D super-resolution is indicated.

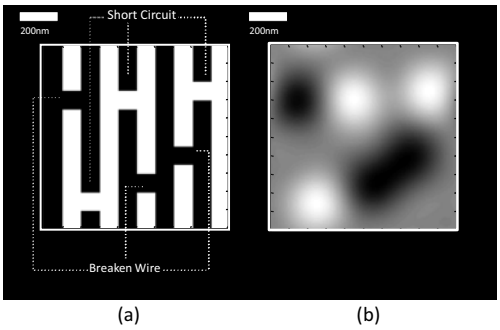

Fig. 8. (a) Short circuit and broken wires on line & space pattern
(b) Normal imaging of *NA*0.95

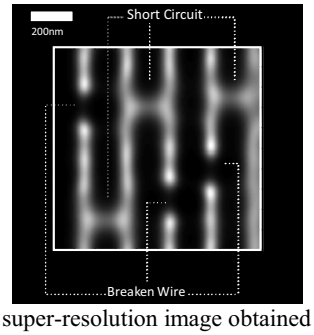

Fig. 9. The 2D super-resolution image obtained by simulation

4. EXPERIMANTAL EQUIPMENT FOR 2D SUPER-RESOLUTION

4.1. Construction of experimental equipment

Experimental equipment based on the proposed method was constructed for the verification of the proposed 2D super-resolution method. Fig. 10 and Fig. 11 show a schematic diagram of the experimental equipment. The following features must be attained by experimental 2D super-resolution equipment. First, two orthogonal standing wave illuminations must be generated on the sample. This is achieved by the optical system of 4 incident light directions as shown in Fig. 10. Second, each standing wave illumination must be able to shift on a nanoscale. PZTs attached to mirror 5 and 6 in Fig. 10 give a phase difference between the 2 beams and enable this feature. Dark-field scattered light detection is also a necessary feature for sensitive detection of defects. This is achieved by an optical system by which incident light enters from outside the objective lens (Fig. 11). A photograph of the experimental apparatus is shown in Fig. 12. Table 2 shows the parameters of the equipment. An objective lens of comparatively low *NA* which allows us to clearly verify the proposed method is used.

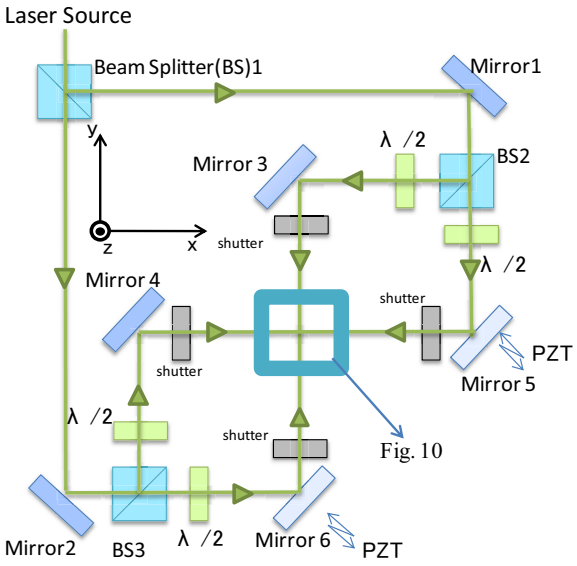

Fig. 10. Schematic diagram of optical system of 4 incident light directions (top view)

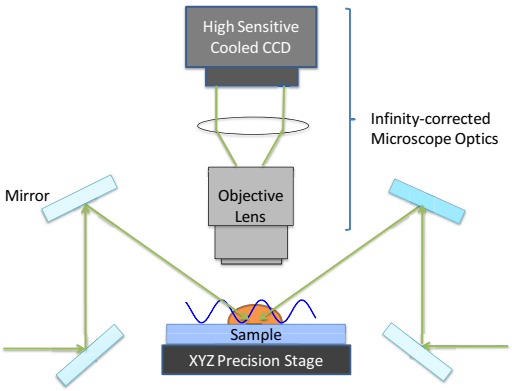

Fig. 11. Schematic diagram of dark-field scattered light detection system (side view)

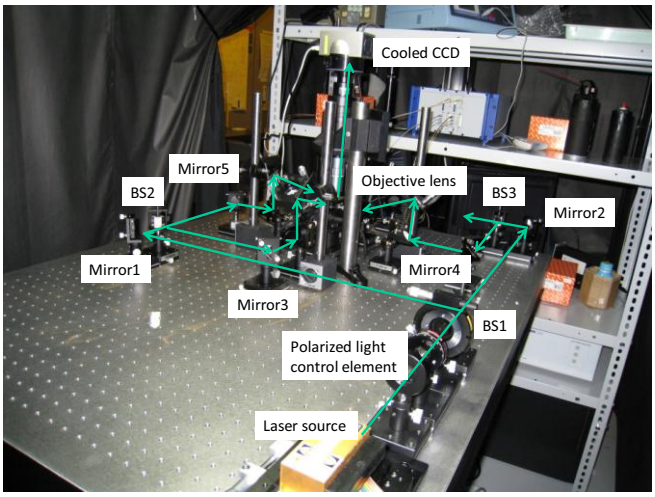

Fig. 12. Photograph of experimental equipment

Table 2. Parameters of the experimental apparatus

Wavelength of source	532nm
Pitch of standing wave illumination	266nm~350nm
Objective lens	*NA* 0.55 ×100
Rayleigh limit	590nm
Resolution of standing wave illumination shift	0.8nm
CCD pixel size	8.3μm × 8.3 μm

4.2. Verifying function of generating and shifting standing wave illumination using moiré stripe

A functional verification of the constructed equipment for generating and shifting standing wave illumination was carried out. The constructed equipment could not resolve a pattern of standing wave illumination because of low *NA*. So, the generated standing wave illumination was indirectly checked by moiré stripe. A schematic diagram of the moiré stripe is shown in Fig. 13. The pitch and the direction of the moiré stripe are determined from pitches of periodic structure and of standing wave illumination; the angle between the periodic structure and standing wave illumination also contributed to the moiré stripe. The relations between them are shown at expression (1), (2). Using the periodic structure, which pitch is known, and the observed data of the moiré stripe, the pitch and direction of the standing wave illumination can be estimated.

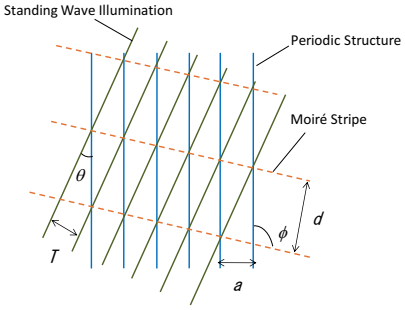

Fig. 13. The schematic diagram of moiré stripe

$$d = \frac{aT}{\sqrt{a^2 + T^2 - 2aT\cos\theta}} \quad (1)$$

$$\sin\phi = \frac{b\sin\theta}{\sqrt{a^2 + T^2 - 2aT\cos\theta}} \quad (2)$$

As a periodic structure, an L&S pattern of known size made by a semiconductor process is employed. The schematic diagram of the 220nm L&S pattern is shown in Fig. 14(a). Fig. 14(b) shows the 220nm L&S pattern (above) and the 200nm L&S pattern (below) illuminated by incident light from the top down. The L&S patterns are not resolved in Fig. 14(b). The sample of Fig. 14(c) is the same as that sample of Fig. 14(b). In this case, however, incident light has entered from two directions, up and down. The L&S patterns are also not resolved, but moiré stripes are observed. This means a standing wave is generated on the sample. The pitch of the standing wave illumination is calculated as 270nm, and the striped pattern of the standing wave is almost horizontal in direction. It was also confirmed that Moiré stripes were observed when incident light entered from the right and the left, and a standing wave in an almost vertical direction was generated. The pitch of the standing wave was calculated as 270nm, too. It is confirmed that two orthogonal standing waves could be generated by the constructed apparatus.

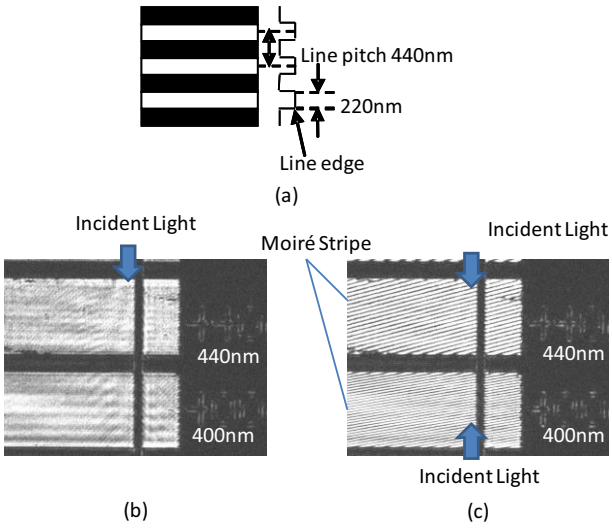

Fig. 14. (a) Schematic diagram of an L&S pattern
(b) Observed image of an L&S pattern (one incident light)
(c) Observed images (incident light directions are up & down)

Moreover, the function of the shifting standing wave illumination is verified as described below. As shown in Fig. 15, when the PZT was driven, a shift in the appearance of the Moiré stripe was confirmed. This shift also confirmed indirectly that the standing wave had shifted.

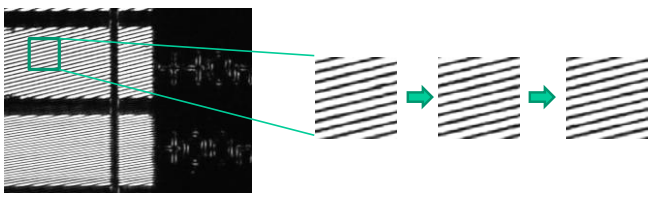

Fig. 15. Moiré stripe shift by driving PZT

5. 2D SUPER-RESOLUTION EXPERIMENT

A sample which has a 200nm L&S pattern, 3 attached foreign particles and carbon contamination [8] was employed for 2D super-resolution experiment. Fig. 16(a) shows SEM images of the sample. A schematic diagram of the sample is shown in Fig. 16(b). Fig. 16(c) shows images of the sample observed by the equipment when incident light entered from the left. The 200nm L&S pattern in this image is not resolved, and the positions of attached foreign particles and carbon contamination are unclear due to low *NA*. Then a 2D super-resolution experiment was carried out on the sample. The experimental setup is defined in Table 3.

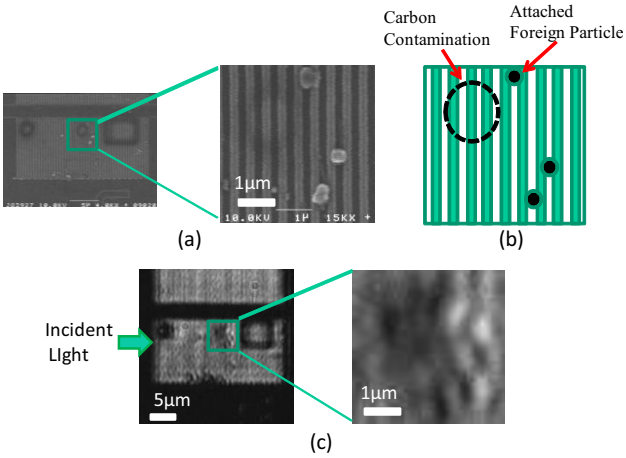

Fig. 16. Images of the sample (a) obtained by SEM
(b) The schematic diagram (c) obtained by the equipment

Table 3. Experimental setup

Pitch of standing wave illumination	270nm
Shift step size	8.3nm
Shift times	x 100 y 100
Iteration times	400

Fig. 17 and Fig. 18 shows examples of modulated scattered light images of the sample by standing wave illumination shift. Incident light directions are right & left in Fig. 17, and up & down in Fig. 18. Changes in the scattered light images of the sample by standing wave illumination shift were observed.

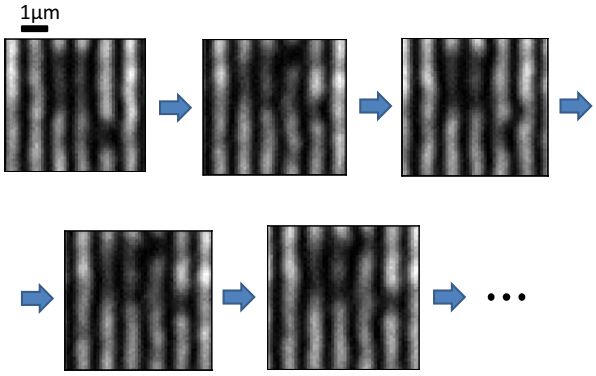

Fig. 17. Examples of modulated scattered light images by standing wave illumination shift (incident light directions are right & left)

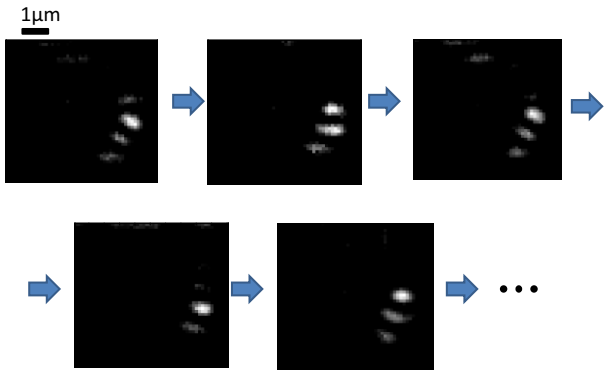

Fig. 18. Examples of modulated scattered light images by standing wave illumination shift (incident light directions are up & down)

2D super-resolution post processing was carried out by using these modulated scattered light images. The 2D super-resolution image of the sample is shown in Fig. 19(b). The structure, which was not resolved in the image before super-resolution post-processing (Fig. 19(a)), is resolved in Fig. 19(b). In Fig. 19(b), the edges of the 200nm L&S pattern are clearly resolved, and positions of the attached foreign particles and carbon contamination become clearer. However, a quantitative survey of the relation between the steps of the re-constructed image and the presence of a foreign body in the wiring is needed.

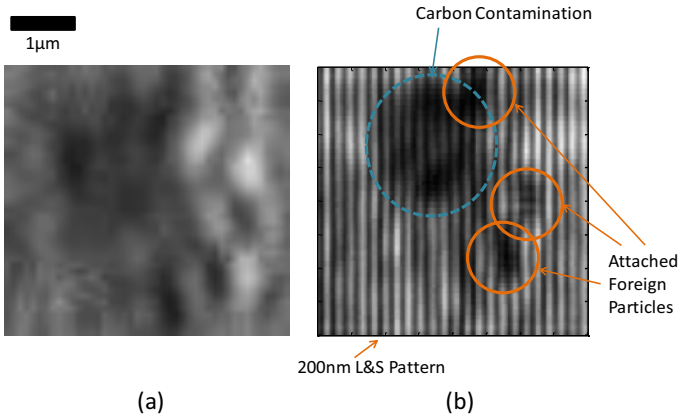

Fig. 19. Images of the sample
(a) before super-resolution post-processing
(b) after 2D super resolution.

6. CONCLUSIONS

To achieve 2D super resolution in super-resolution optical defect inspection of a semiconductor wafer surface, we proposed a method of 2-direction standing wave illumination shift. For verification of the feasibility of the proposed method, we carried out a computer simulation based on Fourier optics and made the following discoveries.

As the result of 2D super-resolution reconstruction for discrete punctate scattered objects, we confirmed that the configuration of scattered objects which can't be resolved by uniform illumination is distinguishable.

Assuming an actual semiconductor pattern, we created a 100nm L&S pattern sample with multiple short circuits and broken wires. As the result of 2D super-resolution reconstruction, the structure of the line & space pattern and positions of short circuits and broken wires were detected.

To verify the proposed 2D super-resolution method experimentally, an experimental apparatus was constructed. This equipment has following features.

Two orthogonal standing wave illuminations can be generated on the sample;

Each standing wave illumination can shift in nanoscale;

It is a dark-field scattered light detection system.

A 2D super-resolution experiment was carried out on the constructed apparatus. As the result of the experiment, a structure having a 200nm L&S pattern with attached foreign particles and carbon contamination, which could not be resolved by uniform illumination, became distinguishable.

In future work, we will make a quantitative assessment of resolution under 2D super resolution, predict the resolution limit of this method theoretically, and verify our prediction experimentally.

ACKNOWLEDGEMENT

This work was partially supported by a Grant-in-Aid for Scientific Research by the Japanese Ministry of Education, Culture, Sports, Science and Technology (Grant No.18656041) and The Kurata Memorial Hitachi Science and Technology Foundation.
The author (One of the authors (R.K.)) was supported through the Global COE Program, "Global Center of Excellence for Mechanical Systems Innovation," by the Ministry of Education, Culture, Sports, Science and Technology.

REFERENCES

[1] "International Technology Roadmap for Semiconductors, Metrology (2008 update)", Semiconductor Industry Association
[2] H. Nishioka, S. Takahashi, K. Takamasu, Proc. of IMEKO World Congress, 12,TC2, 2006.
[3] S. Uski, H. Nishioka, S. Takahashi, K. Takamasu, SPIE International Symposium on Optmechatronic Technologies 2005, (2005), pp60490C-1~60490C-11.
[4] Mark A. Schulze, Martin A. Hunt, Edgar Voelkl, Joel D. Hickson, William Usry, Randall G. Smith, Robert Bryant and C. E. (Tommy) Thomas Jr., Proc. SPIE's Advanced Microelectronic Micromanufacturing, 27-28 February 2003
[5] George W. Mulholland and Thomas A. Germer, Proc. the Government Microcircuits Applications and Critical Technologies (GOMACTech) Conference, March 31 to April 3, 2003
[6] Kenji Watanabe, Shunji Maeda, Tomohiro Funakoshi and Yoko Miyazaki, Hitachi Review Vol. 54, No. 1, pp22-26, 2005
[7] Volker Westphal and Stefan W. Hell, PHYSICAL REVIEW LETTERS, No.143903, 2005
[8] A. E. Vladár and M.T.Postek, Microsc Microanal 11(Suppl2),2005